

# Nanostructuring lithium niobate substrates by focused ion beam milling

F. Lacour, N. Courjal, M.-P. Bernal \*, A. Sabac, C. Bainier, M. Spajer

*Université de Franche-Comté, Institut FEMTO-ST (UMR 6174), Département d'Optique P.M. Duffieux, 25030 Besançon Cedex, France*

Received 18 May 2004; accepted 14 July 2004

## Abstract

We report on two novel ways for patterning lithium niobate (LN) at submicronic scale by means of focused ion beam (FIB) bombardment. The first method consists of direct FIB milling on  $\text{LiNbO}_3$  and the second one is a combination of FIB milling on a deposited metallic layer and subsequent RIE (Reactive Ion Etching) etching. FIB images show in both cases homogeneous structures with well reproduced periodicity. These methods open the way to the fabrication of photonic crystals on  $\text{LiNbO}_3$  substrates. © 2004 Elsevier B.V. All rights reserved.

PACS: 85.40.Ux; 42.70.Qs; 77.84.Dy

Keywords: Nano-structuring; Lithium niobate; Focused ion beam; Reactive ion etching

## 1. Introduction

The recent development of integrated photonic crystals within planar waveguides can help implementing compact devices with fully integrable functions [1–3]. In these devices the light is confined into the crystal by a classical waveguide construction. Lithium niobate (LN) is a suitable material for 2D photonic crystals because of its high refractive index. Moreover, its high electro-optic coefficient and its low optical losses make this material very adequate for optical communication systems. Therefore, the perspective of fabricating miniature electro-optical and all-optical LN devices is attracting the research on  $\text{LiNbO}_3$  nanostructuring [4,5]. However, the obtention of good nanometric optical structures in  $\text{LiNbO}_3$  continues to be a difficult task due to its well-known resistivity towards standard machining techniques like wet etching [6].

In this paper, we report on two alternative methods based on focused ion beam bombardment (FIB) to produce photonic band gap structures on  $\text{LiNbO}_3$  substrates with a spatial resolution of 70 nm. The high resolution and the ability to drill holes directly from the sample surface make FIB milling one of the best candidates for designing good optical quality patterns at submicrometer scale [7]. The only constraint is that the sample surface must be metallised and grounded to avoid charge accumulation. Firstly, we describe the method for directly etching the LN substrate by FIB milling through the metal. This method has been already employed to etch sub-micrometric one-dimensional structures in  $\text{LiNbO}_3$  [8]. The second related method is based on RIE etching after FIB milling of the metal layer which behaves as a mask. The advantage of this alternative solution is a lower exposure time. Another expected advantage would be a good replication of the mask shape in the whole hole depth. In both cases, the fabricated submicronic patterns are characterized by FIB imaging.

Before describing the two nanostructuring methods, we present the calculated conditions to obtain a photonic band gap for  $\text{LiNbO}_3$  substrates.

\* Corresponding author. Tel.: +33 3 81 66 64 10; fax: +33 3 81 66 64 23.

E-mail address: [maria-pilar.bernal@univ-fcomte.fr](mailto:maria-pilar.bernal@univ-fcomte.fr) (M.-P. Bernal).

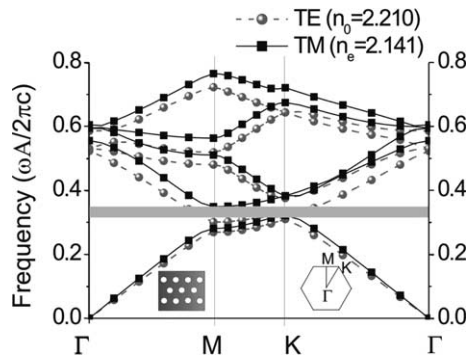


Fig. 1. TE and TM band structure for 2D triangular array.

## 2. Numerical study

Numerical calculations are carried out using the commercial software BandSolve. For a wavelength  $\lambda = 1.55 \mu\text{m}$ , the ordinary and extraordinary indexes of the Z-cut  $\text{LiNbO}_3$  substrate are assumed to be  $n_o = 2.2151$  and  $n_e = 2.1410$ , respectively. According to our calculations, a 2D triangular lattice of holes can yield to a total TM photonic bandgap if the diameter  $D$  of the holes is larger than  $0.4p$ , where  $p$  is the triangular lattice period. The ratio  $D/p$  should be as large as possible in order to benefit from a large photonic band gap, but it cannot exceed 0.5 for technological reasons. Indeed, the walls between holes could collapse for diameters larger than  $0.5p$ . Fig. 1 shows the band diagram obtained in the case  $D/p = 0.5$ . As it can be seen from the figure, the structure yields to a total TM-photonic band gap for frequencies between  $0.321p/(2\pi c)$  and  $0.349p/(2\pi c)$ . The difference from the calculation of Massy et al. [9] is probably the difference between the refraction index that are chosen in both cases. Having

shown the existence of a photonic band gap in lithium niobate, we have investigated the means of nanostructuring it.

## 3. Experimental

The two fabrication processes are schematically shown in Fig. 2. The first method—Fig. 2(a)—is based on a direct etching of the  $\text{LiNbO}_3$  substrate by FIB milling. The second one—Fig. 2(b)—uses the FIB to create the metallic mask and the pattern is then transferred to the  $\text{LiNbO}_3$  substrate by RIE. In both cases the sample area is  $1 \text{ cm}^2$  and the thickness  $500 \mu\text{m}$ . A Cr layer is deposited by electron gun evaporation (Balzer, B510) and grounded with a conductive paste before introduction into the FIB vacuum chamber ( $= 2 \times 10^{-6} \text{ Torr}$ ). In the case of direct FIB writing the thin Cr metal layer (150 nm) does not modify significantly the etching efficiency. In the second case a thicker Cr layer (250 nm) is deposited.

The metal-coated substrates are milled using a focused ion beam column (Orsay Physics—LEO FIB4400 for the case of FIB milling only—Fig. 2(a)—and a FEI Dual Beam Strata 235 for the milling of the metallic mask—Fig. 2(b). This method could be directly compared with e-beam lithography. The advantage of FIB patterning of the metallic mask is its ability to selectively remove and deposit material without the use of the additional process step of developing a resist layer.

In the first case (Fig. 2(a)) we have fabricated an array of  $4 \times 4$  circular holes with 540 nm diameter and  $1 \mu\text{m}$  periodicity.  $\text{Ga}^+$  ions are emitted with a current of  $2 \mu\text{A}$  and accelerated by a voltage of 30 kV. The ions are focused with electrostatic lenses on the sample with a

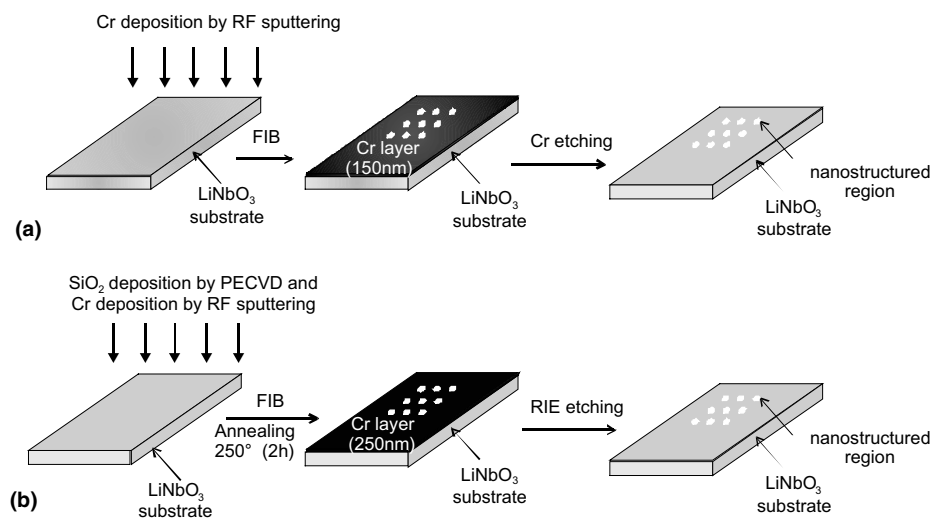


Fig. 2. (a) Process steps used to achieve nanostructures on  $\text{LiNbO}_3$  substrates by FIB milling only. (b) The metallic mask is done by FIB milling and the structuring of  $\text{LiNbO}_3$  is done by RIE.

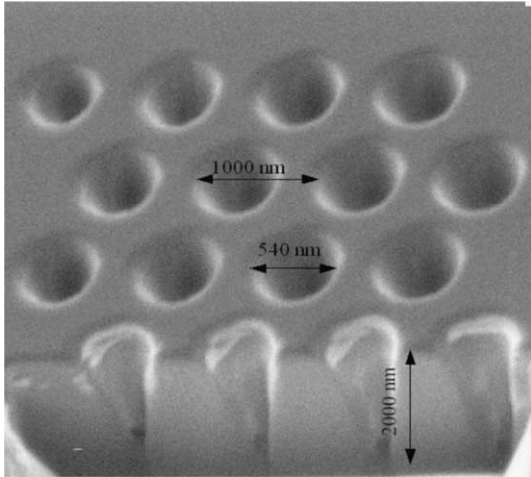


Fig. 3. FIB image of the FIB-etched  $\text{LiNbO}_3$   $4 \times 4$  array of circular holes.

probe current of 66 pA. The pseudo-Gaussian-shaped spot size is estimated to be 70 nm on the target. The focused ion beam is scanned on the sample by a computer-controlled deflection field to produce the desired pattern (Elphy Quantum from Raith). A FIB-image cross-section of the cavities is shown in Fig. 3. In order to see the etching depth the sample is tilted  $30^\circ$  with respect to the FIB axis. As it can be seen from the image, the  $4 \times 4$  array exhibits well defined circular holes. The achieved etching depth is approximately  $2 \mu\text{m}$  and the etching time was 12 min. At  $1 \mu\text{m}$  deep the hole diameter is about 432 nm. This conical etching shape is due to material redeposition on the sidewalls while milling. In order to reduce the redeposition there are two possible solutions. If the FIB electronics is fast enough (Elphy Quantum is limited to 300 KHz) and the spot size small enough one can scan along the hole sidewalls longer and less on the bottom of the pit. A second possibility that we plan to implement in our system is to use gas assisted milling. In particular,  $\text{XeF}_2$  could help to remove Nb from the etched substrate decreasing then the redeposition.

The etching depth and the real hole diameter can differ from the designed ones and this difference depends on the  $\text{Ga}^+$  dose. This can be clearly seen in Fig. 4(a) and (b) where this dependence has been measured. It is clear from the graphs that as the milling time is increased, the etching depth increases but with a subsequent increase in the hole diameter due to beam aberrations. In particular, an increase of almost 30% in the hole diameter and of 40% in the etching depth has been measured as the  $\text{Ga}^+$  dose is increased by a factor of 4 from the initial value ( $4 \times 10^4 \mu\text{A s/cm}^2$ ). Therefore, for practical uses one should start with a designed hole diameter slightly smaller than the desired one.

The second related process requires lower etching time since the desired photonic structure is fabricated

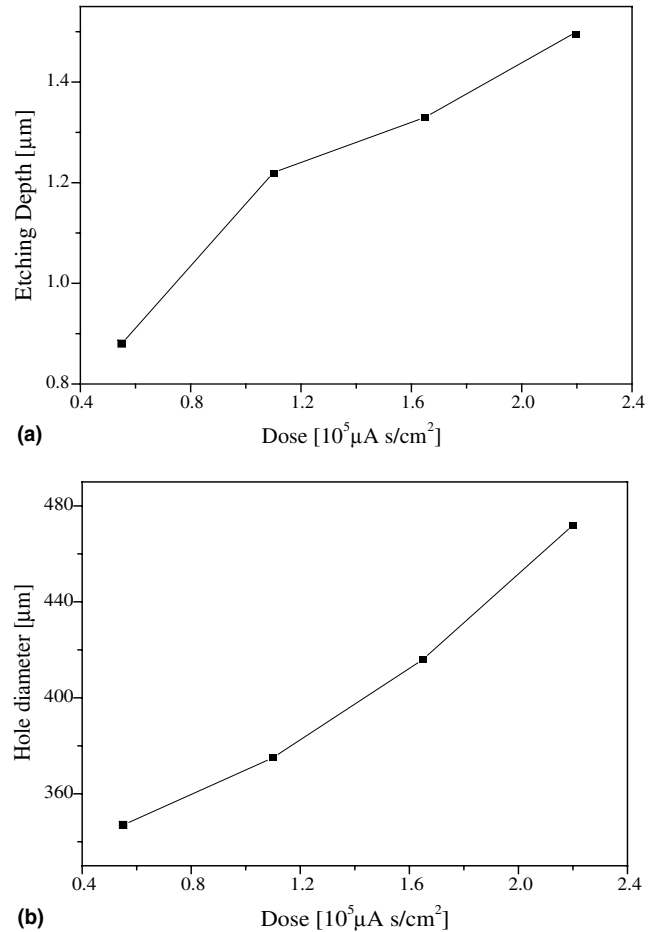


Fig. 4. (a) Dependence of the hole depth with respect to the  $\text{Ga}^+$  ion dose with a cross-section at the first hole-line plane. (b) Dependence of the hole diameter with respect to the  $\text{Ga}^+$  dose.

at once. In this case, the FIB bombardment is used to pattern a  $\text{SiO}_2$ -Cr mask previously deposited on the LN substrate, as depicted in Fig. 2(b). The first step consists in depositing a 100 nm thick layer of  $\text{SiO}_2$  by Plasma Enhanced Chemical Vapor Deposition (PECVD). A 250 nm thick chrome layer is then deposited on the substrate by sputtering. The metal is used as a mask for the RIE, while the silica layer prevents the diffusion of Chrome into the substrate during the RIE plasma processing and the increase of the optical losses. This layer is not needed in the case of direct FIB milling since the etching is done locally and the damaged area is defined by the FIB beam size. The samples are annealed at  $250^\circ\text{C}$  during 2 h to release stress. The  $\text{SiO}_2$ -Cr mask is then nanostructured by FIB patterning, with a current of the sample of 100 pA. An exposure time of 3.75 s is typically required to etch a 250 nm diameter circular hole, which is 11 times lower than the one required in the first process.

The pattern (an array of  $24 \times 20$  cylindrical holes) is finally transferred to the substrate by RIE. The relevant parameters of this process are detailed in Table 1. It

Table 1  
Parameters of the RIE process

LiNbO <sub>3</sub>	Pressure (mbar)	SF <sub>6</sub> flow (sccm)	RF power (W)	Etching rate (nm/min)	LiNbO <sub>3</sub> /Cr selectivity
Z-cut	3	10	150	50	0.25

can be noticed that this process requires a very low pressure and a high RF power. In these conditions, the etch rate of the mask is comparable to the etching rate of the substrate. In order to improve the selectivity of etching between the mask and the LiNbO<sub>3</sub> substrate, we start the process with an exposition of the target to a O<sub>2</sub> ionic plasma (pressure = 100  $\mu$ bar, power = 60 W). The 250 nm thick layer of chrome is then more resistant to the SF<sub>6</sub>-RIE. The selectivity of the mask is thus estimated to be 1:5 compared to the LiNbO<sub>3</sub> substrate (while the etching selectivity was measured to be of 1:2 without the O<sub>2</sub> ionic plasma). The etching rate of the Z-cut substrate is measured to be 50 nm/min. This process is applied to fabricate a triangular lattice of holes with  $D = 250$  nm and  $D = 130$  nm diameters and

$p = 2*D$  periodicity. Fig. 5(a) and (b) exhibit the SEM images of the holes after FIB milling and 10 min of RIE etching. Fig. 5(a) shows holes with good reproducibility. The etching depth is measured to be 500 nm. Fig. 5(b) shows that the 130 nm diameter holes were transformed into 130 nm diameter rods after RIE etching, while the 250 nm diameter holes were well preserved. This is due to a higher etching rate along the sides of the triangular lattice than in the triangle center when the holes are very close to each other. We can infer from these results that the fabrication of small holes ( $D < 200$  nm) requires lower RF-power to preserve the initial feature.

#### 4. Conclusion

In this work we have presented two alternative techniques to fabricate submicrometric patterns in LiNbO<sub>3</sub> by means of a FIB milling or a combination of FIB milling and RIE etching. In particular, 500 nm-diameter circular holes were etched by FIB milling obtaining an etching depth of 2  $\mu$ m. Material redeposition starts to be a problem for etching depths larger than 1  $\mu$ m. A  $24 \times 20$  array of 250 nm-diameter circular holes and 500 nm periodicity was realized using an alternative method in which the metallic mask is fabricated by FIB milling and the LiNbO<sub>3</sub> etching is obtained by SF<sub>6</sub> RIE. In this case, the etching depth in LiNbO<sub>3</sub> is around 500 nm and is limited by the metallic thickness of the mask. Work is in progress to optimize the RIE etching in view of obtaining a higher etching depth. An optical characterization of the patterns is also in progress.

As opposed to the process based on ferro-electric domain inversion, the presented methods are more suitable for implementing nanostructures on both X-cut and Z-cut substrates.

We are currently working on the theoretical analysis and the fabrication of active LiNbO<sub>3</sub> 2D-photonics crystals. In order to operate at 1.55  $\mu$ m our calculations show that we must have a triangular geometry of cylindrical holes of 259 nm diameter and 519 nm periodicity.

#### Acknowledgments

The authors want to thank Jack Vendeville (FEMTO-ST, Université de Franche-Comté, Besançon) and Eloïse

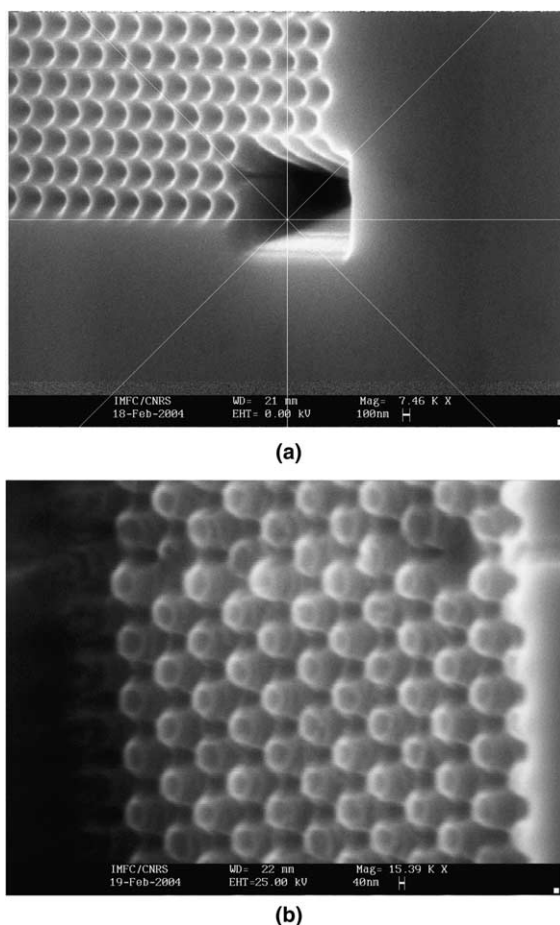


Fig. 5. SEM image of the LiNbO<sub>3</sub> substrate covered by 250 nm of Chrome after FIB milling and 10 min of RIE etching. (a)  $D = 250$  nm. (b)  $D = 130$  nm.

Devaux (Laboratoire des Nanostructures, ISIS, Université Louis Pasteur, Strasbourg) for technical assistance and Jean-Yves Rauch (FEMTO-ST, Université de Franche-Comté, Besançon) for fruitful discussions.

## References

- [1] M. Kamp, T. Happ, S. Mahnkopf, G. Duan, S. Anand, A. Forchel, *Physica E* 21 (2004) 802.
- [2] J. Zimmermann, M. Kamp, A. Forchel, R. Marz, *Optics Communication* 230 (2004) 387.
- [3] L. Wu, M. Mazilu, J.-F. Gallet, T.F. Krauss, *Photonics and Nanostructures—Fundamentals and Applications* 1 (2003) 31.
- [4] C. Restoin, S. Massy, C. Darraud-Taupiac, A. Barthelemy, *Optical Materials* 22 (2003) 193.
- [5] V. Foglietti, E. Ciani, D. Pezzeta, C. Sibilis, M. Marangoni, R. Osellame, R. Ramponi, *Microelectronic engineering* 67–68 (2003) 742.
- [6] EMIS Data Reviews Series No. 5, *Properties of Lithium Niobate* (IN-SPEC, London and New York, 1989).
- [7] C.G. Bostan, R.M. de Ridder, V.J. Gadgil, L. Kuipers, A. Driessen, *Proceedings Symposium IEE/LEOS Benelux Chapter*, Enschede, The Netherlands, 2003.
- [8] S. Yin, *Proc. IEEE* 87 (1999) 1962.
- [9] S. Massy, C. Restoin, C. Darraud, A. Barthelemy, *Structures périodiques bidimensionnelles sur  $\text{LiNbO}_3$  et  $\text{H}_x\text{Li}_{1-x}\text{NbO}_3$  réalisées par bombardement par faisceau d'électrons*, JNOG 2003, Valence (France).